# A STUDY OF OPTICAL BAND GAP AND ASSOCIATED URBACH ENERGY TAIL OF CHEMICALLY DEPOSITED METAL OXIDES BINARY THIN FILMS

F. N. C. ANYAEGBUNAM, C. AUGUSTINE[*]
*Department of Physics/Geology/Geophysics, Alex Ekwueme Federal University Ndufu-Alike Ikwo, Nigeria*

In this paper, we present the influence of post deposition annealing and varying concentration on the optical properties of NiO, ZnO and $Co_3O_4$ thin films, with emphasis on the effect of growth parameters on optical band gap and Urbach energy. Increasing the concentration of each of the precursor solutions decreased the band gap from 3.85eV to 3.75eV for NiO film samples, 3.90eV to 3.85eV for $Co_3O_4$ film samples and increased from 3.85eV to 3.88eV for ZnO film samples. With respect to annealing temperature, no clear trend was observed. The fundamental absorption edge shifted toward a lower photon energy with respect to concentration for NiO and $Co_3O_4$ thin films whereas it shifted to higher photon energy for ZnO thin films. An inverse relation between band gap energy and Urbach energy was found. The range of band gaps are suitable for applications in various solar architecture, optoelectronics and high frequency applications.

## 1. Introduction

Metallic oxides occupy a prominent place in thin film research due to their verse optical, structural and physiological characteristics which include high temperature superconductivity, ferroelectricity, ferromagnetism, piezoelectricity, semiconductivity [1]. Optical, optoelectronic, magnetic, electric, thermal, electrochemical, catalytic and sensor properties [1, 2]. Other notable optical characteristics are high optical transmittance, [3, 4]. The diversity emanates from the more complex crystal and electronic structures of metal oxides in comparison to other classes of materials [5]. The elegancy of the metal oxides are found in the oxidation states, coordination numbers, symmetry, crystal-field stabilization, density, stoichiometry and acid-base surface properties that they exhibit [5]. These properties made them to find applications in photodiodes, phototransistors, photovoltaics, transparent electrodes, liquid crystal displays, IR detectors and anti-reflection coating [6].

The nickel oxide (NiO) thin films is a transition metal oxide with excellent chemical and thermal stability [7, 8]. It has potential applications in such areas as electro-chromic display devices, anti-ferromagnetic layers, solar thermal absorber and as cathode material for alkaline batteries [9-11]. Some other interesting electronic properties of NiO thin film include its wide band gap range of 3.6-4.0eV [12] and its p-type conductivity which make it a favourable material for electronic device applications [8, 13]. Zinc oxide (ZnO) is an important ll-Vl compound semiconductor with a wide band gap of about 3.37eV at room temperature [14]. ZnO has been used for the fabrication of light emitting diodes, photo detectors, piezoelectric cantilever, gas sensors, buffer layer in solar cell and in photonic crystals [15-20]. Cobalt oxide ($Co_3O_4$) is an important p-type semiconductor with direct optical band gaps at 1.48eV and 2.19eV [21], $Co_3O_4$ has been investigated extensively as promising materials in gas-sensing and solar energy absorption and as an effective catalyst in environmental purification and chemical engineering [22,

---

[*]Corresponding author: emmyaustine2003@yahoo.com

23]. In addition, $Co_3O_4$ thin film has been widely studied for its application as lithium ion battery electrodes, catalysts, ceramic pigments, field-emission materials and magnetic materials [24-27].

Many workers have investigated the optical properties of NiO, ZnO and $Co_3O_4$ thin films but only few focused on the optical band gap, Urbach tail width and their varaiation with film thickness and post deposition temperature. In our previous study, we investigated the behaviour of optical band gap and Urbach tail width with annealing temperature [28]. In this study, NiO, ZnO and $Co_3O_4$ thin films were prepared by chemical bath deposition, the band gap energy was estimated, and its dependence on concentration and deposition temperature were investigated. The Urbach tail width was also estimated and its relation with concentration, post deposition temperature and band gap energy were analyzed .

## 2. Experimental

NiO, ZnO and $Co_3O_4$ thin films have been synthesized by chemical bath deposition technique. The microscopic glass slides used as substrates prior to deposition were soaked in concentrated hydrochloric acid for 24 hours, removed and washed with foam-sponge in ethanol and finally rinsed in distilled water. Thereafter, they were then drip dried in air. The degreased, cleaned surface has the advantage of providing nucleation centers for the growth of the films, hence, yielding highly adhesive and uniformly deposited films.

### 2.1 Synthesis of NiO thin films

NiO thin films were prepared from a solution of nickel sulphate [$NiSO_4$].The precursor was dissolved in distilled water with addition of 5ml of ammonia solution as stabilizer. The precursor concentration, which served as a starting solution, was varied from 0.2M to 0.4M. The resulting solution was stirred at room temperature using a magnetic stirrer for 10 minutes to yield a clear and pale blue transparent solution. The mixture for the deposition was placed in an electric oven at temperature of $65^{o}C$ for 3 hours. The chemical kinetics of the reaction is shown below:

$$NiSO_4 .6H_2O + NH_3 \rightleftharpoons [Ni (NH_3)_6]^{2+} + (SO_4)^{2-}$$
$$[Ni (NH_3)_6]^{2+} \rightleftharpoons Ni^{2+} + 6NH_3$$
$$Ni^{2+} + 2OH \rightleftharpoons Ni (OH)_2$$
$$Ni (OH)_2 \longrightarrow NiO + H_2O$$
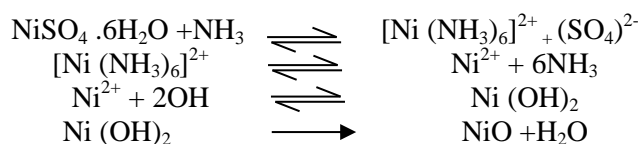
### 2.2 Synthesis of ZnO thin films

ZnO thin films were grown from a solution containing 0.2M-0.4M concentrations of hydrated zinc nitrate (Zn $(NO_3)_2 \cdot 6H_2O$) and 1M hexamine mixed appropriately in distilled water. The chemical bath containing the reaction mixture was subjected to temperature of $65^{o}C$ in an oven for 5 hours. The chemical reaction is shown below:

$$C_6H_{12}N_4 + 6H_2O \longrightarrow 6HCHO + 4NH_3$$
$$NH_3 + H_2O \longrightarrow NH_4^{+} + OH^{-}$$
$$2OH^{-} + Zn^{2+} \longrightarrow ZnO + H_2O$$
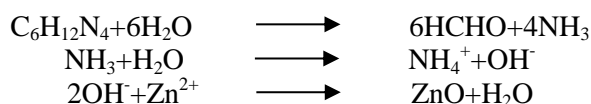
### 2.3 Synthesis of $Co_3O_4$ thin films

$Co_3O_4$ thin films have been synthesized using cobalt acetate tetra hydrates and methanol precursor solutions and stirred vigorously at 60°C for 1 h, leading to the formation of light pink color powder. The prepared powder was sintered at various temperatures ranging from 100°C - 200°C with a fixed annealing time of 1 hr in an ambient air to obtain $Co_3O_4$ thin films. The growth mechanism of $Co_3O_4$ as formulated by [29] is shown below:

$$Co (CH_3COO)_2.4H_2O + 2CH_3-OH \longrightarrow CoO (OH)_2 + 2CH_3COOCH_3 + 4H_2O$$
$$CoO (OH)_2 \longrightarrow Co_3O_4 + H_2O$$
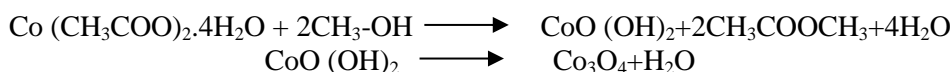
**2.4 Thin film characterization**

Thermo scientific GENESYS 10S model UV-VIS spectrophotometer was used to determine the transmittance of the deposited films in the wavelength range of 300-1000 nm.

## 3. Results and discussion

Transmittance spectra for un-annealed NiO, ZnO and $Co_3O_4$ thin films at 0.2M and 0.4M concentration recorded in the wavelength range 300–900 nm are indicated in Figs. 1 and 2 respectively. The plots depicted a sharp rise in transmittance near the band edge attributed to good crystallinity of the films [30]. Fig.1 shows a narrow range of variation of transmittance for the three oxides layers. Increasing the molarity of the precursor solution from 0.2M to 0.4M, a wide variation of transmittance was observed as shown in Fig.2, except for $Co_3O_4$ thin film, where a considerable decrease in transmittance is observed by increasing the molarity of the precursor solution from 0.2M to 0.4M. At 0.2M concentration, ZnO films transmit higher in the wavelength range 400nm-1000nm compared to other oxide layers (Fig.1) whereas at 0.4M concentration, $Co_3O_4$ thin films exhibited maximum transmittance in the entire wavelength region. Figs. 3 and 4 depict the plots of transmittance against wavelength of films annealed at $100^oC$ for 0.2M and 0.4M respectively. As indicated in Fig.3, a slight decrease in transmittance is observed for the three oxide layers after annealing at $100^oC$. The same trend is observed when annealing temperature increased to $150^oC$ and $200^oC$ as shown in Figs.5 and 7 respectively. The decrease in transmittance could be attributed to the increase in particle size due to thermal annealing. In our earlier study, we reported a decrease in transmittance with increasing annealing temperature for heterojunction thin films [31-34]. Such decrease in transmittance as a result of thermal annealing has also been reported by other research groups [35]. As indicated in Figs. 4, 6 and 8 for annealed at $100^oC$, $150^oC$ and $200^oC$ respectively for 0.4M concentration, NiO and ZnO thin films showed significant increase in transmittance exhibiting a maximum in the infrared region. Survey of literature showed that other authors have reported similar transmittance results [36, 37]. In all the films, the absorption edge shifted to greater wavelength which is indicative of the fact that the band gap decreased. The properties of high transmittance makes the films good materials for optical coatings.
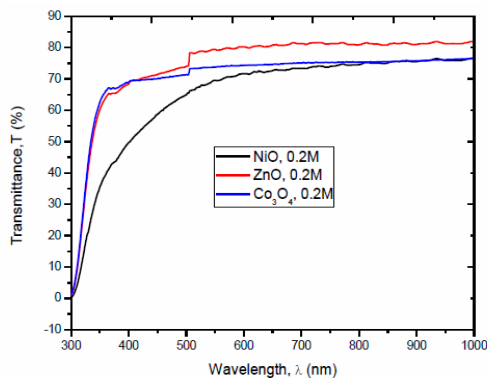


*Fig.1. Plots of T against λ for as-deposited at 0.2M*
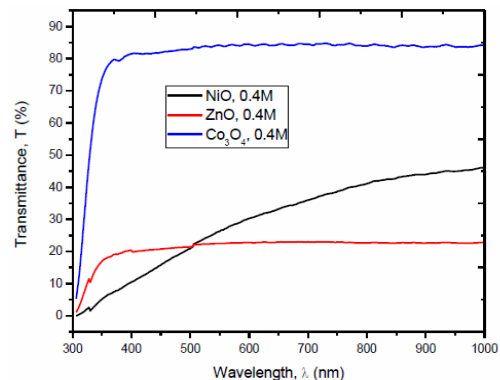


*Fig. 2. Plots of T against λ for as-deposited at 0.4M*
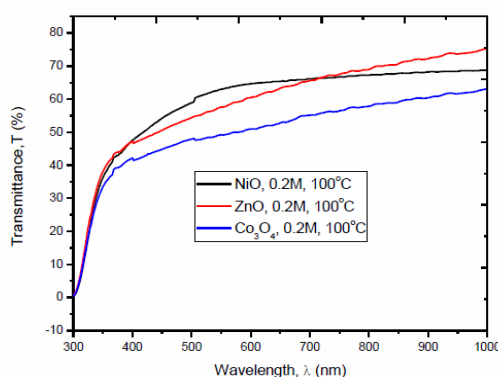
Fig. 3. Plots of T against λ for 0.2M annealed at 100°C
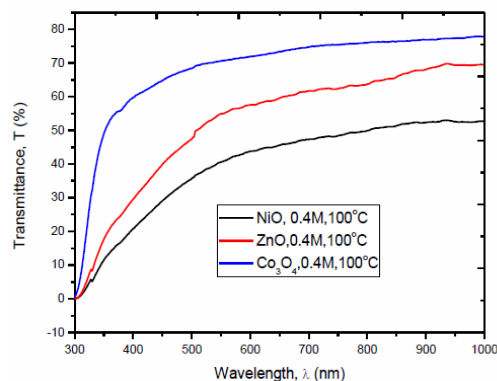


Fig. 4. Plots of T against λ for 0.4 annealed at 100°C
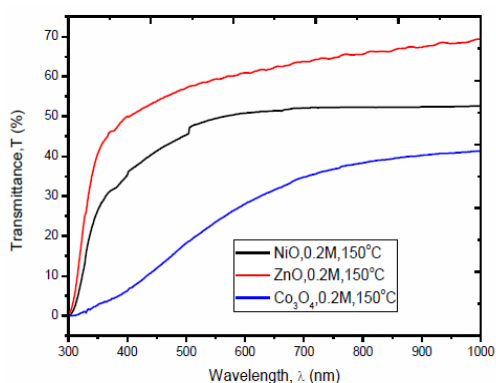


Fig. 5. Plots of T against λ for 0.2 annealed at 150°C
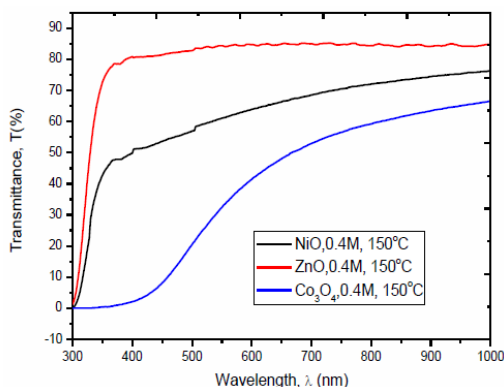


Fig. 6. Plots of T against λ for 0.4 annealed at 150°C
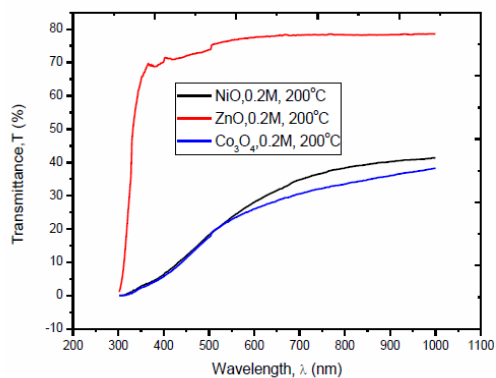


Fig. 7. Plots of T against λ for 0.2 annealed at 200°C
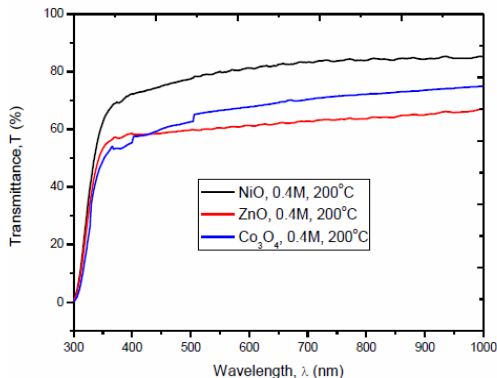


Fig. 8. Plots of T against λ for 0.4 annealed at 200°C

Direct energy gap was determined by plotting a graph between $(\alpha h v)^2$ versus $h v$ and extrapolation of straight line to $(\alpha h v)^2 = 0$ gives the direct band gap values of different concentrations of NiO, ZnO and $Co_3O_4$ thin films for as-deposited and annealed at 100°C, 150°C and 200°C as seen in Figs. 9-16. The calculated band gap values are listed in Tables 1 and 2 for 0.2M and 0.4M respectively at different annealing temperatures. Generally, there is lack of trend with annealing temperature with respect to the band gaps. However, some of the film samples exhibited some form of correlation with increase in annealing temperature. With respect to concentration, a clear trend was observed for all the film samples. For NiO thin films, the band gap decreased from 3.85eV to 3.75eV as concentration increased from 0.2M to 0.4M. The band gap of ZnO thin film decreased from 3.90eV to 3.85eV with increase in concentration whereas $Co_3O_4$ thin films depicts an increase in band gap from 3.85eV to 3.88eV. Obtained band gap values for

NiO and ZnO thin films are in good agreement with results carried out in literature [38-44]. Obtained band gap values of $Co_3O_4$ thin films are higher than those reported in literature [45, 46]. The higher band gaps recorded for $Co_3O_4$ thin films could be as a result of experimental conditions. The Tauc's relation was used to calculate the values of the band gap using equation (1) [47].

$$(\alpha h v)^n = A(h v - E_g)$$ (1)

where A is band edge parameter and value of n determines the nature of optical transition (n = ½ indicates direct transition and n = 2 indicates indirect transition).
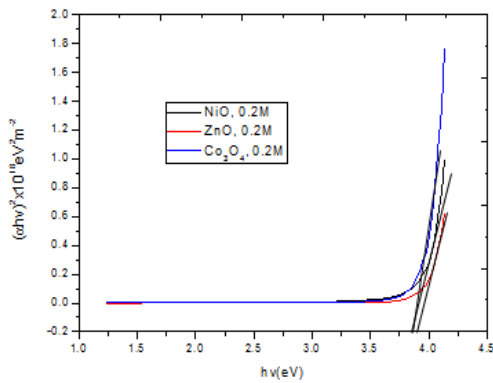


Fig. 9. Plots of $(\alpha h v)^2$ versus hv for as-deposited samples at 0.2M
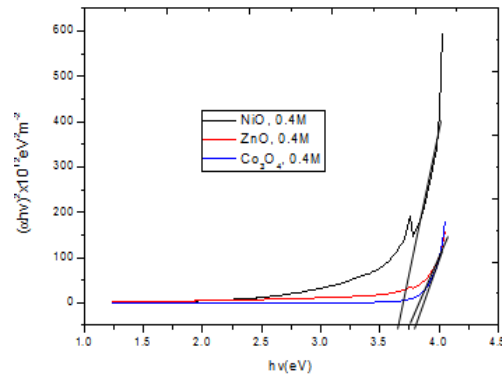
Fig.10. Plots of $(\alpha h v)^2$ versus hv for as-deposited samples at 0.4M

Table 1. Band gap values of film samples deposited at 0.2M at different annealing temperature

| Sample | Conc. (M) | $E_g$ (eV) before annealing | $E_g$ (eV) after annealing at | | |
|---|---|---|---|---|---|
| | | | 100°C | 150°C | 200°C |
| NiO | 0.2 | 3.85 | 3.80 | 3.85 | 3.65 |
| ZnO | 0.2 | 3.90 | 3.70 | 3.90 | 3.85 |
| $Co_3O_4$ | 0.2 | 3.85 | 3.90 | 3.55 | 3.60 |

Table 2. Band gap values of film samples deposited at 0.4M at different annealing temperature

| Sample | Conc. (M) | $E_g$ (eV) before annealing | $E_g$ (eV) after annealing at | | |
|---|---|---|---|---|---|
| | | | 100°C | 150°C | 200°C |
| NiO | 0.4 | 3.75 | 3.78 | 3.85 | 3.75 |
| ZnO | 0.4 | 3.85 | 3.60 | 3.90 | 3.85 |
| $Co_3O_4$ | 0.4 | 3.88 | 3.75 | 2.90 | 3.65 |
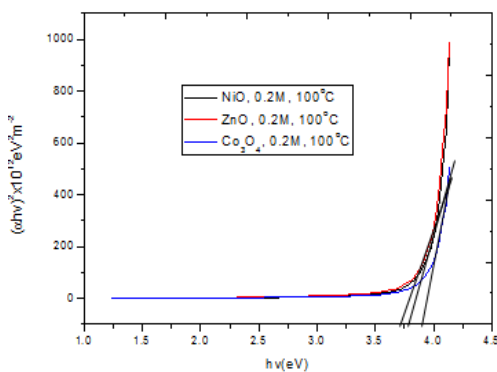


Fig.11. Plots of $(\alpha h v)^2$ versus hv of samples for annealed at 100°C at 0.2M
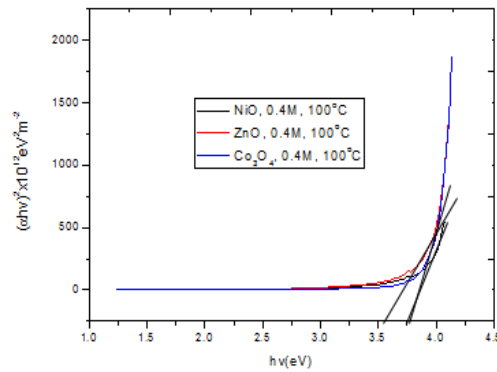
Fig.12. Plots of $(\alpha h v)^2$ versus hv of samples for annealed at 100°C at 0.4M
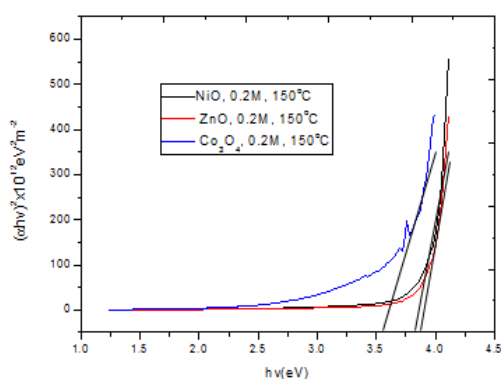
Fig.13. Plots of (αhv)² versus hv of samples for
annealed at 150°C at 0.2M
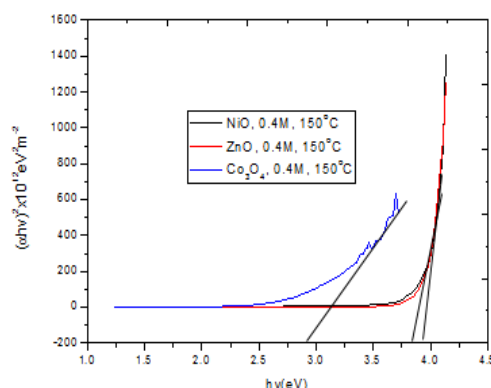


Fig.14. Plots of (αhv)² versus hv of samples for
annealed at 150°C at 0.4M
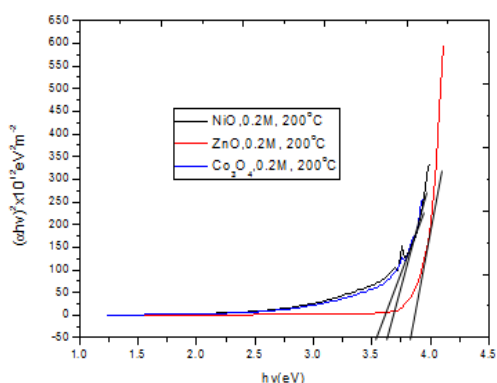


Fig.15. Plots of (αhv)² versus hv of samples for
annealed at 200°C at 0.2M
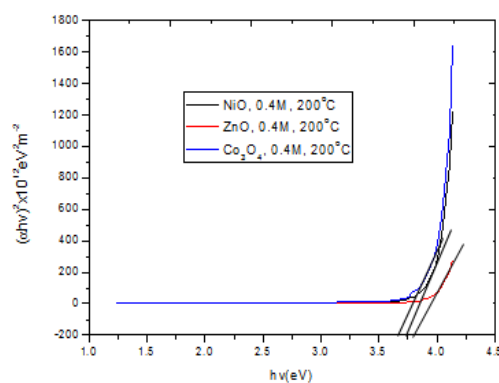


Fig.16. Plots of (αhv)² versus hv of samples for
annealed at 200°C at 0.4M

A disorder, so called Urbach tails, which is related to width of the localized states available in the optical band gap of the NiO, ZnO and $Co_3O_4$ thin films was studied for further investigation. This width of the localized states, is related directly to a similar exponential tail for the density of states near band edges and can be expressed by the temperature and spectral dependence of absorption coefficient [48].

$$\alpha\left(hv, T\right) = \alpha_0 . \exp\left[\sigma \frac{\left(hv - E_0\right)}{KT}\right] = \alpha_0 . \exp\left[\frac{hv - E_0}{E_u\left(T\right)}\right] \tag{2}$$

where $E_u$ is the Urbach energy which is equal to the energy width of the absorption edge, $\sigma$ is the steepness parameter of the absorption edge, $\alpha_0$ and $E_0$ are the coordinates of the convergence point of the Urbach ''bundle''. The Urbach energy $E_u$ are well described in the framework of the Einstein model [49, 50].

$$E_{g\ (T)}^* = E_{g\ (0)}^* - S_g^* K\theta_E \left[\frac{1}{\exp\left(\frac{\theta_E}{T}\right) - 1}\right] \tag{3}$$

$$E_u = \left(E_u\right)_0 + \left(E_u\right)_1 \left[\dfrac{1}{\exp\left(\dfrac{\theta_E}{T}\right)-1}\right] \tag{4}$$

where $E_g^{*}{}_{(0)}$ is the energy gap at 0K, $S_g^{*}$, $\left(E_u\right)_0$ and $\left(E_u\right)_1$ are the constant values, $\theta_E$ is the Einstein temperature which corresponds to the average frequency of phonon excitations of non-interacting oscillations. These equations can be compressed into an empirical formula proposed by [51, 52].

$$\alpha = \alpha_o \exp\left(\dfrac{hv}{E_u}\right) \tag{5}$$

where $\alpha_o$ is a constant, $E_u$ denotes an energy which is constant or weakly dependent on temperature and is often interpreted as the width of the tail of localized states in the band gap. The exponential tail appears because disordered and amorphous materials produce localized states extended in the band gap [53]. The band tail energy or Urbach energy ($E_u$) can be obtained from the slope of the straight line of plotting $\ln(\alpha)$ against the incident photon energy ($hv$). Fig. 7 shows the variation of ln ($\alpha$) versus photon energy ($hv$) for the films. *Eu* values were calculated from reciprocal of the straight line slopes, as shown in the Fig. 7, and illustrated in Table 3. As can be seen from Table 3, the energy band gap is averaged in 3.68–3.60 eV. The decrease in the optical band gap with precursor concentration may be attributed to the increase in grain size and decrease in structural disorder in the films as observed from Urbach energy analysis. In general it was shown that the band gap of all samples is inverted to Urbach energy.

*Table 3. Urbach energy tail values of film samples deposited at 0.2M at different annealing temperature*

| Sample | Conc. (M) | $E_g$ (eV) before annealing | $E_g$ (eV) after annealing at | | |
|---|---|---|---|---|---|
| | | | 100°C | 150°C | 200°C |
| NiO | 0.2 | 2.75 | 3.00 | 3.10 | 1.40 |
| ZnO | 0.2 | 3.80 | 2.85 | 3.35 | 3.30 |
| $Co_3O_4$ | 0.2 | 3.15 | 3.30 | 2.65 | 1.75 |

*Table 4. Urbach energy tail values of film samples deposited at 0.4M at different annealing temperature*

| Sample | Conc. (M) | $E_g$ (eV) before annealing | $E_g$ (eV) after annealing at | | |
|---|---|---|---|---|---|
| | | | 100°C | 150°C | 200°C |
| NiO | 0.4 | 1.25 | 2.85 | 3.15 | 3.10 |
| ZnO | 0.4 | 2.60 | 2.40 | 3.40 | 3.30 |
| $Co_3O_4$ | 0.4 | 3.30 | 3.25 | 1.13 | 3.10 |
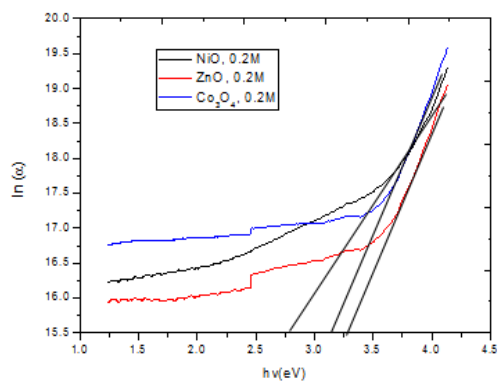
*Fig.17. Plots of $\ln(\alpha)$ versus hv of samples for as-deposited at 0.2M*
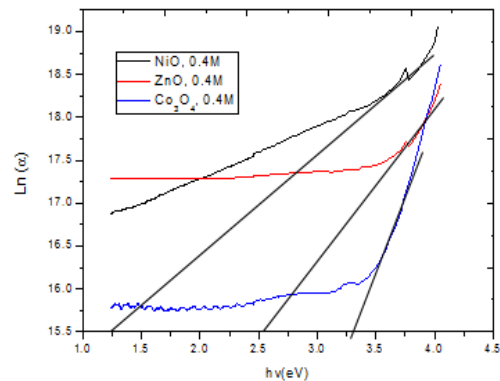


*Fig.18. Plots of $\ln(\alpha)$ versus hv of samples for as-deposited at 0.4M*
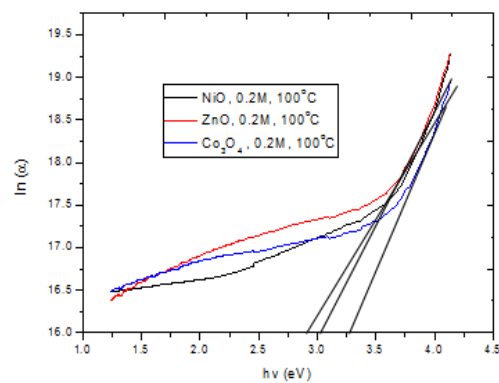


*Fig.19. Plots of $\ln(\alpha)$ versus hv of samples for annealed at $100^oC$ at 0.2M*
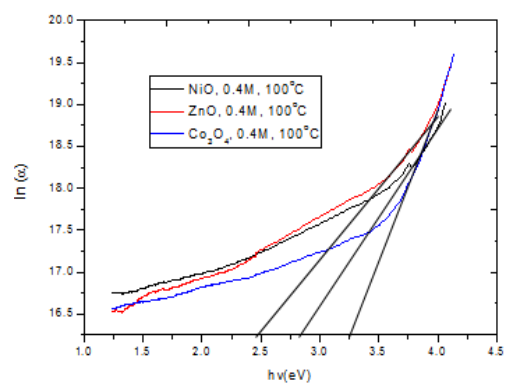


*Fig. 20. Plots of $\ln(\alpha)$ versus hv of samples for annealed at $100^oC$ at 0.4M*
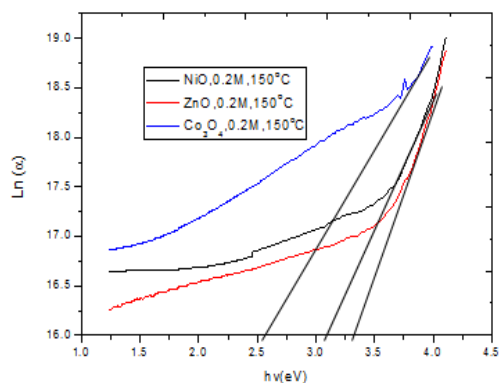


*Fig.21. Plots of $\ln(\alpha)$ versus hv of samples for annealed at $150^oC$ at 0.4M*
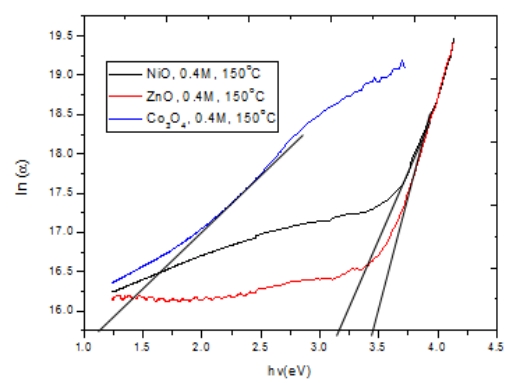


*Fig. 22. Plots of $\ln(\alpha)$ versus hv of samples for annealed at $150^oC$ at 0.4M*
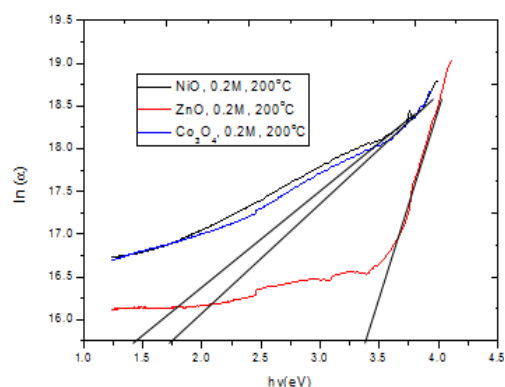
*Fig. 23. Plots of* $\ln(\alpha)$ *versus hv of samples for annealed at 100°C at 0.2M*
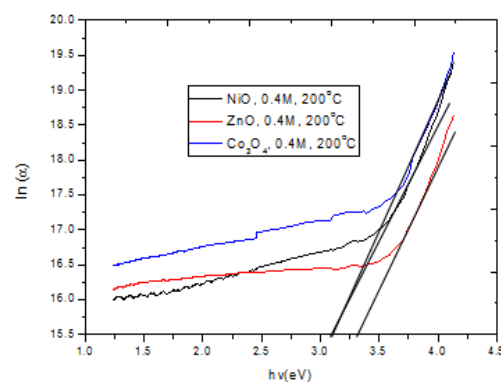


*Fig. 24. Plots of* $\ln(\alpha)$ *versus hv of samples for annealed at 200°C at 0.4M*

## 4. Conclusions

Chemical bath deposition process has been employed for deposition of ZnO. NiO and $Co_3O_4$ thin films from chemical bath containing varied concentrations of the principal precursor solutions. The films were annealed within the temperature range 100-200°C. The transmittance measurements were made using spectrophotometer from which the band gap and Urbach energy were determined. With respect to concentration, the band gap is in the range of 3.75-3.85eV for NiO film samples, 3.85-3.90eV for ZnO films and 3.85-3.88eV for $Co_3O_4$ thin films. After annealing, the band gap for NiO and ZnO film samples lie in the range 3.65-3.85eV and 3.70-3.85eV respectively while that of $Co_3O_4$ films is 3.85-3.90eV. The Urbach energy varied inversely to the band gap. The band gap values are suitable for use in solar cell fabrication, optoelectronic and high frequency applications.

## References

[1] Q. X. Jia, T. M. Mccleskey, A. K. Burrell, G. E. Collis, H. Wang, A. D. Q. Li, S. R. Foltyn, Nature Materials **3**, (2004).
[2] L. Vayssieres, Int. J. Nanotechnol. **1**, (2004).
[3] M. Ortega, G. Santana, A. Morales-Acevedo, Superficies y Vacio. **9**, 294 (1999).
[4] R. S. Rusu, G. I. Rusu, J. Optoelectron Adv. M. **7**(2), 823 (2005).
[5] B. A. Ezekoye, V. A. Ezekoye, P. O. Offor, S. C. Utazi, International Journal of Physical Sciences **8**(31), 1597 (2013).
[6] D. S. Dhawale, A. M. More, S. S. Latthe, X. Y. Rajpure, C. D. Lokhande, Appl. Surf. Sci. **254**, 3269 (2008).
[7] H. Chen, Y. Lu, W. Hwang, Surface and Coating Technology **198**, 138 (2005).
[8] A. E. Ajuba, S. C. Ezeugwu, P. U. Asogwa, F. I. Ezema, Chalcogenide Letters **10**(7), 573 (2010).
[9] A. Fuchs, M. Bogner, K. Shangal, R. Winter, T. Dell, I. Eisele, Sens. Actuators B. Chem. **47**, 145 (1998).
[10] T. Miki, K. Yoshimura, S. Tanemura, Jpn. J. Appl. Phys. **34**, 240 (1995).
[11] A. Tomozawa, F. Fujii, H. Torii, R. Takayama, Jpn. J. Appl. Phys. **35**, 1328 (1996).
[12] T. Minami, H. Sati, S. Takata, T. Y. Yamada, Thin Solid Films **27** (1995).
[13] S. R. Kriss, M. Liberatic, V. M. Grazioli, S. Turchini, P. Luchis, S. Vateri, C. Carbone, Journal of Magnetism and Magnetic Materials **310**, 8 (2007).
[14] T. Soki, Y. Hatanaka, D. C. Look, Applied Physics Letters **76**(22), 3257 (2000).
[15] Y. Lin. C. R. Gorla, S. Linng, N. Emanetoglu, Y. Tor, H. Shen, M. Wraback, Journal of Electronic Materials **29**(1), 69 (2000).
[16] V. R. Shinde, T. P. Gujar, C. D. Lokhande, Sensors and Actuators H **120**(2), 551 (2007).

[17] A. Ennaoui, S. Siebentrith, M. Ch. Lux-Steiner, W. Riedl, F. Karg, Solar Energy Materials and Solar Cells **67**(1-4), 31 (2002).
[18] Y. Chen, D. Bagnall, T. Yao, Materials Science and Engineering B **75**(2-3), 190 (2000).
[19] S. Liang, H. Sheng, Y. Liu, Z. Hio, Y. Lu, H. Shen, Journal of Crystal Growth **225**, 110 (2001).
[20] M. H. Koch, P. Y. Timbrell, R. N. Lamb, Semiconductor Science and Technology **10**(11), 1523 (1995).
[21] A. O. Gulino, P. Dapporto, P. Rossi I. Fragalà, Chemistry of Materials **15**(20), 3748 (2003).
[22] X. W. Lou, D. Deng. J. Y. Lee, J. Feng and L. A. Archer, Advanced Materials **20**(2), 258 (2008).
[23] S. Lian, E. Wang, L. Gao, L. Xu, Materials Letters **61**(18), 3893 (2007).
[24] D. Zou, C. Xu, H. Luo, L. Wang, T. I. Ying, Materials Letters **62**(12-13), 1976 (2008).
[25] P. Poizot, S. Laruelle, S. Grugeon, L. Dupont, J. M. Tarascon, Nature **407**(6803), 496 (2000).
[26] B. Varghese, T. C. Hoong, Y. W. Zhu, M. V. Reddy, V. R. Chowdari, T. S. Wee, B. C. Vincent, C. T. Lim, C. Sow, General & Introductory Materials Science **17**(12) 1932 (2007).
[27] J. Jiang, L.-C. Li, Materials Letters **61**(27), 4894 (2007).
[28] C. Augustine, Journal of optoelectronic and Biomedical Materials **10**(4), (2018).
[29] V. Patil, P. Joshi, N. Chougule, S. Sen, Soft Nanoscience Letters **2**, 1 (2012).
[30] M. A. Al-Sabayleh, Univ. J. Sci. Med. Engg. **20**, 17 (2008).
[31] C. Augustine, M. N. Nnabuchi, F. N. C. Anyaegbunam, A.N. Nwachukwu, Digest Journal of Nanomaterials and Biostructures **12**(2), 523 (2017).
[32] C. Augustine, M. N. Nnabuchi, Journal of Ovonic Research **13**(4), 233 (2017).
[33] C. Augustine, M. N. Nnabuchi, Journal of Non-Oxide Glasses **9**(3), (2017).
[34] C. Augustine, M. N. Nnabuchi, F. N.C Anyaegbunam, C. U. Uwa, Chalcogenide Letters, **14**(8), 321 (2017).
[35] P. E. Agbo, G. F. Ibeh, S. O. Okeke, J. E. Epke, Communications in Applied Sciences **1**(1), 38 (2013).
[36] P. A. Nwofe, P. E. Agbo, Journal of Non-Oxide Glasses **9**(1), 9 (2017).
[37] J. S. Cruz, D. S. Cruz, M. C. Arenas-Arrocena, F. D. M. Flores, S. A. M. Hernandez, Chalcogenide Letters **12**(5), 277 (2015).
[38] R. Barir, B. Benhaoua, S. Benhamida, A. Rahal, T. Sahraoui, R. Gheriani, Journal of Nanomaterials, 101155 (2007).
[39] S. Nandy, B. Saha, M. K. Mitra, K. K. Chattopadhyay, Journal of Materials Science **42**(14), 5766 (2007).
[40] F. I. Ezema, A. B. C. Ekwealor, R. U. Osuji, Superficies y Vacio **21**(1), 6 (2008).
[41] U. M. Patil, R. R. Salunkhe, K. V. Gurav, C. D. Lokhande, Applied Surface Science **255**, 2603 (2008).
[42] R. J. Hong, J. B. Huang, H. B. He, Z. X. Fan, J. D. Shao, Applied Surface Sciences **242**(3-4), 346 (2005).
[43] S. Benramache, A. Rahal, B. Benhaoua, Optik **124**, 663 (2013).
[44] S. Zhao, L. Yang, Y. Zhou, Optik **122**, 960 (2011).
[45] V. Patil, P. Joshi, M. Chougule, S. Sen, Soft Nanoscience Letters **2**, 1 (2012).
[46] A.O. Gulino, P. Dapporto, P. Rossi, I. Fragala, Chemistry of Materials **15**(20), 3748 (2003).
[47] C. D. Lokhande, B. R. Sankapal, S. Mane, H. M. Pathan, M. Muller, M. Giersig, V. Ganesan, Appl. Surf. Sci. **193**, 1 (2002).
[48] F. Urbach, APS Journals, Phys. Rev. **92**, 1324 (1953).
[49] M. Beaudoin, A. J. G. DeVries, S. R. Johnson, H. Laman, T. Tiedje, APS Journals, Appl. Phys. Lett. **70**, 3540 (1997).
[50] Z. Yang, K. P. Homewood, M. S. Finney, M. A. Harry, K. J. Reeson, AIP, J. Appl. Phys. **78**, 1958 (1995).
[51] V. Bilgin, S. Kose, F. Atay, I. Akyuz, Mater. Chem. Phys. **94**,103 (2005).
[52] Y. Natsume, H. Sakata, T. Hirayama, Phys. Stat. Sol. (A) **148**, 485 (1995).
[53] S. J. Ikhmayies, R. N. Ahmad-Bitar, Journal of Materials Research and Technology **2**(3), 221 (2013).